Available online at www.sciencedirect.com

SCIENCE DIRECT®

Polymer 46 (2005) 8634–8640

polymer

www.elsevier.com/locate/polymer

Poly(*N*-vinyl carbazole)-functionalized single-walled carbon nanotubes: Synthesis, characterization, and nanocomposite thin films

Wei Wang, Yi Lin, Ya-Ping Sun*

Department of Chemistry and Laboratory for Emerging Materials and Technology, Clemson University, P.O. Box 340973, Clemson, SC 29634-0973, USA

Received 18 April 2005; received in revised form 27 May 2005; accepted 13 June 2005
Available online 15 August 2005

Abstract

A poly(*N*-vinyl carbazole) (PVK) copolymer containing pendant hydroxyl groups was synthesized for the functionalization of single-walled carbon nanotubes (SWNTs) under typical reaction conditions for the esterification of the nanotube-bound carboxylic acids. The functionalized nanotube samples, soluble in common organic solvents, were characterized by using optical absorption, Raman, and several microscopy techniques. The presence of ester linkages was supported by the results from chemical defunctionalization in hydrolysis that recovered insoluble SWNTs. The shared solubility of the functionalized nanotube samples with PVK enabled the wet-casting of high-quality PVK-SWNT nanocomposite thin films for an evaluation of their enhanced charge dissipation under illumination.

Keywords: Nanocomposites; Nanotubes; Photoconductivity

1. Introduction

Polymeric photoconductive materials have found many important applications [1]. Among well-known photoconductive polymers is poly(*N*-vinyl carbazole) (PVK), which is commonly used with a dopant to increase charge generation efficiency in the visible and beyond. A variety of dopants have been developed, such as nanoscale semiconductors and fullerenes [2,3]. Recently, the use of single-walled carbon nanotubes (SWNTs) in nanocomposites with photoconductive polymers has attracted much attention [4–12]. The broad absorption of SWNTs over the visible and near-IR wavelength regions may allow their use as nanoscale dopant for broadband photosensitization. The nanotubes above certain concentration in polymeric nanocomposites are also expected to form a percolation network for enhanced electrical conductivity, which may facilitate the charge transportation in photoconductors such as PVK-SWNT.

A significant challenge in the preparation of PVK-SWNT and other polymeric nanocomposites is the homogeneous dispersion of nanotubes in the polymer matrix, which is hindered by the bundling and insolubility of the nanotubes. In fact, the dispersion is particularly important in the fabrication of photoconductive nanocomposites because of the requirement for high optical quality to facilitate efficient light absorption (minimizing light scattering). The recent development in the solubilization of carbon nanotubes has suggested that SWNTs can be de-bundled in solution upon their functionalization, amenable to their homogeneous dispersion into polymer films via simple wet-casting [13–28]. Especially attractive is the use of polymers in the nanotube functionalization that are either identical to or structurally minimally altered from the matrix polymers, thus to ensure full compatibility in the resulting nanocomposites. For example, Hill, et al. functionalized carbon nanotubes with polystyrene copolymers and then dispersed homogeneously the solubilized nanotubes into the polystyrene matrix [16,17]. Similarly, Qu et al. synthesized an amino-terminated oligomeric polyimide to functionalize carbon nanotubes via the amidation of the nanotube surface-bound carboxylic acids. The soluble functionalized nanotube samples were mixed with neat polyimide polymer in solution for the fabrication of high-quality nanocomposite thin films [19].

Here we report on a similar application of the strategy to disperse SWNTs into PVK polymer matrix in a fully

---

* Corresponding author. Tel.: +1 864 656 5026; fax: +1 864 656 5007.
E-mail address: syaping@clemson.edu (Y.-P. Sun).

0032-3861/$ - see front matter © 2005 Published by Elsevier Ltd.
doi:10.1016/j.polymer.2005.06.039

compatible fashion. The nanotubes were functionalized with a PVK-based copolymer containing a small fraction of styrene units bearing pendant hydroxyl groups, which were designed for the esterification of the nanotube surface-bound carboxylic acids. The functionalized SWNTs were found to share solubility with PVK in common organic solvents, which allowed the solution-phase mixing and the subsequent spin-casting of PVK-SWNT nanocomposite thin films. Results from the sample characterization and a qualitative evaluation for enhanced charge dissipation in the nanocomposite under light illumination are presented and discussed.

2. Experimental section

2.1. Materials

p-Chloromethylstyrene (90%), sodium hydride (NaH, 60%, dispersed in mineral oil), and ethylene glycol (99+%) were purchased from Acros, 9-vinyl carbazole and 2,2′-azobis(isobutyronitrile) (AIBN, 98%) from Aldrich, and thionyl chloride ($SOCl_2$) and poly(*N*-vinyl carbazole) (PVK, $M_W = 100{,}000$) from Alfa Aesar. 4-(4′-Vinylphenyl)-3-oxabutanol (VPOB) was synthesized from *p*-chloromethylstyrene and ethylene glycol as previously described [16]. Styrene was obtained from Baker and was carefully distilled before use. Deuterated chloroform for NMR measurements (containing tetramethylsilane as internal standard) was supplied by Cambridge Isotope Laboratories.

The SWNT sample was produced by using the arc-discharge method [29] in Prof A.M. Rao's laboratory at Clemson University. The as-produced sample was purified by the oxidative acid treatment in a procedure already reported in the literature [16]. Briefly, a suspension of SWNTs (500 mg) in aqueous HNO_3 (2.6 M, 100 ml) was refluxed for 48 h, followed by centrifuging to discard the supernatant. The remaining solids were washed repeatedly with deionized water until neutral and then dried under vacuum.

2.2. Measurements

UV/vis/near-IR absorption spectra were recorded on Shimadzu UV3100 and Thermal-Nicolet Nexus 670 FT-NIR spectrometers. Raman spectra were obtained on a Renishaw Raman spectrometer equipped with a 50 mW diode laser source for 785 nm excitation and CCD detector. Mass spectroscopy was conducted on a Bruker Daltonics AutoflexII MALDI-TOF instrument, with 2,5-dihydroxybenzoic acid as the matrix. NMR measurements were performed on a JEOL Eclipse+500 NMR spectrometer. Thermogravimetric analysis (TGA) was carried out on a Mettler-Toledo TGA/SDTA851e system. The gel permeation chromatography (GPC) system consisted of a pump (Shimadzu LC-10AS), a UV–vis detector (Dynamax UV-1), a fluorescence detector (Shimadzu RF-10A$_{XL}$), a reflective index detector (Thermal Separation Products RefractoMonitor IV), and Perkin–Elmer PLgel 10μ mixed columns. Scanning electron microscopy (SEM) images were obtained on a Hitachi S-4700 field-emission SEM system. Transmission electron microscopy (TEM) analyses were conducted on Hitachi HD-2000 TEM/STEM system. Atomic force microscopy (AFM) was performed on a Molecular Imaging PicoPlus system equipped with a multipurpose scanner of maximum scanning area of $100 \times 100\ \mu m^2$. The height analyses of AFM images were assisted by SPIP software distributed by Image Metrology. The electrical charge dissipation experiments were carried out on a John Chubb Instrumentation JCI 155v4 charge decay test unit.

2.3. Poly(N-vinyl carbazole-co-p-(4-(4′-vinylphenyl)-3-oxabutanol)) (PKS)

In a typical experiment, a toluene solution (100 ml) of VPOB (1 g, 5.6 mmol) and 9-vinyl carbazole (10.8 g, 56 mmol) was mixed with a toluene solution (10 ml) of AIBN (92 mg, 0.56 mmol). The mixture was stirred at 80 °C for 12 h under argon protection. After being concentrated, the reaction mixture was precipitated into cold petroleum ether. The solids from filtration were washed with petroleum ether, and then dissolved in chloroform for a repeat of the purification via precipitation. The copolymer PKS was obtained as a white powder (8.35 g, 70% yield). For the molecular weight of PKS, the result of $M_W \sim 12{,}000$ (polydispersity ~ 2.3) from GPC (linear polystyrene standards, THF, 1 ml/min) was supported by that of $M_n \sim 6000$ from MALDI-TOF.

2.4. Functionalization of SWNTs

In a typical experiment (Scheme 1), a purified SWNT sample (75.2 mg) was refluxed in $SOCl_2$ (25 ml) for 24 h, followed by the removal of excess $SOCl_2$ under vacuum. Separately, PKS (500 mg) in a minimal amount of THF was added through a syringe to a slurry of NaH (800 mg) in THF (125 ml) with constant stirring. After refluxing for 2 h, the slurry was mixed with the $SOCl_2$-treated SWNT sample. The mixture was stirred under nitrogen protection at room temperature for 48 h. The suspension thus obtained was centrifuged at 3000*g* to collect the dark-colored supernatant. The solid residue was extracted repeatedly with THF, coupled with centrifugation. All of the soluble fractions were combined, and then the solvent THF was evaporated. The solid sample was re-dissolved in chloroform and precipitated into cold hexane. Upon washing with deionized water and drying under vacuum, the PKS-functionalized SWNT sample was obtained as greyish black powders.

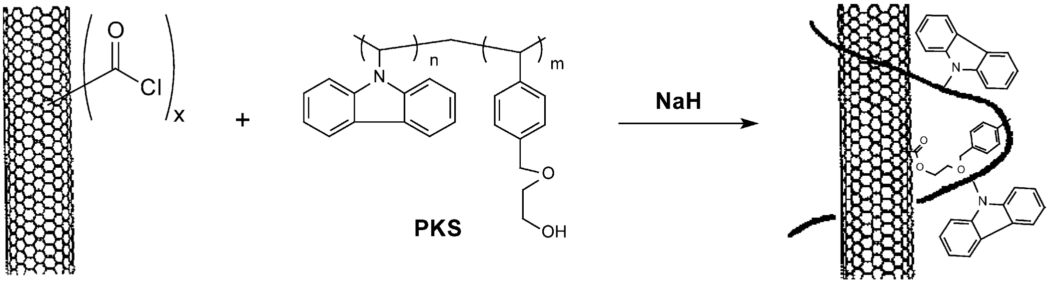

Scheme 1.

2.5. Chemical defunctionalization

In a typical experiment, to a solution of PKS-functionalized SWNT sample in THF (6 mg/ml, 5 ml) was added trifluoroacetic acid (5 ml). The mixture was refluxed under nitrogen protection for 10 h, resulting in the formation of dark-colored precipitates. Upon centrifuging, the solids were collected, washed repeatedly with chloroform, and then dried completely in a vacuum oven for characterization.

2.6. PVK-SWNT nanocomposite films

In a typical experiment for film with a high nanotube content, a solution of PKS-functionalized SWNTs in chlorobenzene (20 mg/ml, 2 ml) was prepared. To the solution was added a PVK homopolymer sample (200 mg). Upon vigorous mixing, the viscous solution was spin-coated (Laurell Model WS-400A-6TFM/LITE) onto a pre-cleaned ITO-coated glass substrate (1 min at 500 rpm, 30 s at 1500 rpm, and then 30 s at 2500 rpm). The resulting thin film was dried in air at 80 °C for 6 h.

3. Results and discussion

The PKS copolymer is majority PVK, with only ~10 mol% VPOB units according to the ^{1}H NMR ($CDCl_3$ as solvent) signal integrations of the methylene protons in VPOB units and the total aromatic protons in the polymer. Since it is known that defects on nanotube surface are converted to carboxylic acids upon oxidative acid treatment [30,31], they may be targeted by the pendant hydroxyl groups in VPOB units to form ester linkages. In the esterification reaction through the acyl chloride route, the presence of excess NaH is apparently necessary [32,33]. It not only serves as an acid trap but also eliminates any trace amount of water in the reaction mixture. In fact, the reaction without NaH was found to be inefficient, with only very limited solubilization of nanotubes under otherwise the same experimental conditions.

The PKS-functionalized SWNT sample is readily soluble in many common organic solvents (such as THF, chloroform, chlorobenzene, DMF, and DMSO, solubility on the order of 0.5 mg/ml) at room temperature to form dark-colored but visually clear solutions (stable for months), in contrast to the colorless solutions of PKS and PVK. The optical absorption spectra (Fig. 1) of the PKS-functionalized SWNT sample were measured in a DMSO solution and also in the solid-state because of the strong solvent interference for the longer wavelength region beyond 1500 nm. The absorption bands at ~1800 and 1000 nm are characteristic of the electronic transitions associated with the first (S_{11}) and second (S_{22}) pairs of van Hove singularities in the density of states for the semiconducting SWNTs, and the weak band at ~700 nm corresponds to the absorption of the metallic SWNTs (M_{11}). Thus, it seems that the electronic structures of SWNTs are preserved upon the functionalization targeting the nanotube surface defect sites. This is consistent with what have already been reported in the literature [16–19,31].

The Raman spectrum of the PKS-functionalized SWNT sample is shown in Fig. 2, where there is obviously overwhelming luminescence interference. The luminescence in functionalized carbon nanotube samples has been attributed to well-passivated nanotube surface defects [34–36], namely that structural defects on nanotubes may act as traps for the photoexcitation energy, and these energy trapping sites may be

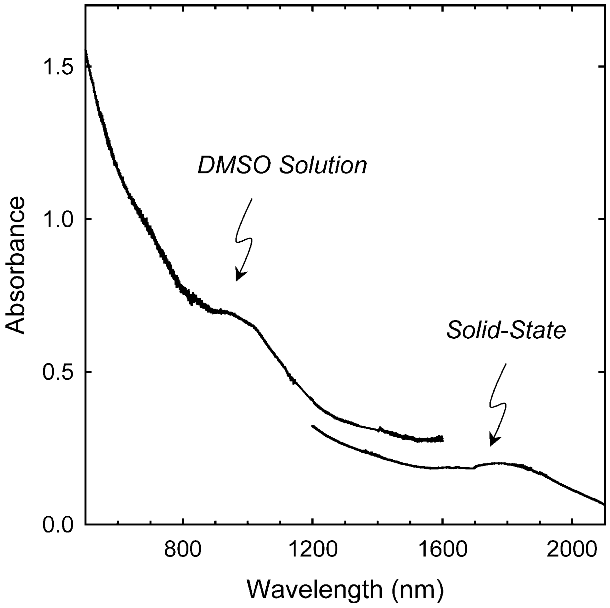

Fig. 1. Optical absorption spectra of the PKS-functionalized SWNT sample.

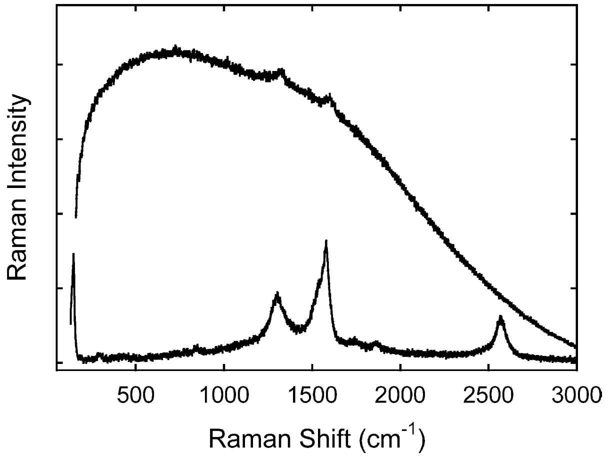

Fig. 2. Raman spectra of the PKS-functionalized SWNT sample before (top) and after (bottom) thermal defunctionalization.

stabilized by the functional groups to be responsible for the observed broad luminescence. As discussed in the literature [37], there is strong experimental evidence suggesting that the functionalization is required for the observation of the nanotube defects-derived luminescence and that a better dispersion of nanotubes in their functionalization enhances the luminescence and, consequently, results in more significant interference in Raman measurements. The correspondence of luminescence enhancement to improved nanotube dispersion is understandable because of the known inter-tube quenching effect associated with the bundling of the nanotubes [34–38]. Thus, the observed overwhelming luminescence interference in the Raman spectrum is an indication that the nanotubes were well-dispersed in the PKS-functionalized SWNT sample. As expected, a removal of the functional groups in the thermal defunctionalization of the functionalized nanotube sample eliminated the luminescence interference, with the Raman spectrum of the resulting sample exhibiting the characteristic SWNT features: D*-band at 2580 cm^{-1}, G-band at 1590 cm^{-1}, D-band at 1310 cm^{-1}, and the radial breathing mode at 167 cm^{-1} (Fig. 2).

The PKS-functionalized SWNTs were evaluated on mica surface in AFM analyses, for which the specimen was prepared by preserving the nanotube dispersion in solution as much as possible. In the preparation, a dilute solution of the PKS-functionalized SWNTs in cholorbenzene was sprayed onto a heated mica substrate to facilitate the desired rapid solvent evaporation. Shown in Fig. 3 is a typical AFM image of the sample. There are apparently abundant nanotubes in the specimen, with their lengths ranging from 100 nm to 2 μm. However, the nanotubes are grouped into features that are 1–2 nm in thickness according to the height analysis (Fig. 3). It may be argued that the functionalized SWNTs are dispersed individually or in thin bundles while in solution, but assembled on surface in the preparation of the specimen due probably to surface tension-related issues and interactions between the polymeric functional groups.

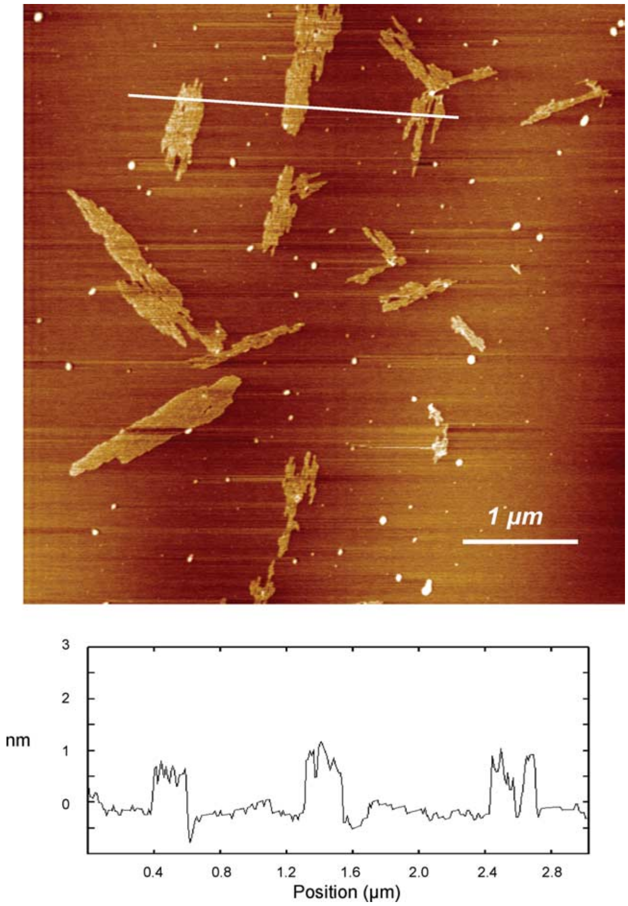

Fig. 3. An AFM image (top) of the PKS-functionalized SWNT sample. The height analysis plot (bottom) is from left to right along the line in the image (results similar for other species in the image).

The PKS-functionalized SWNTs were thermally defunctionalized to allow an estimate of the nanotube content in the sample. In a TGA scan (Fig. 4), the functional groups were removed from the nanotube surface at 500 EC °C in an inert atmosphere, leaving behind mostly clean SWNTs according to the subsequent SEM analysis (Fig. 5). The

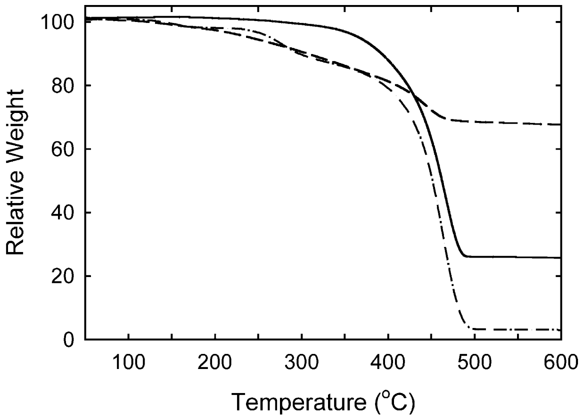

Fig. 4. TGA traces (N_2, 10 °C/min) of the PKS-functionalized SWNT sample (—), the insoluble residue from the functionalization reaction (- - -), and neat PKS polymer (- · - · - ·).

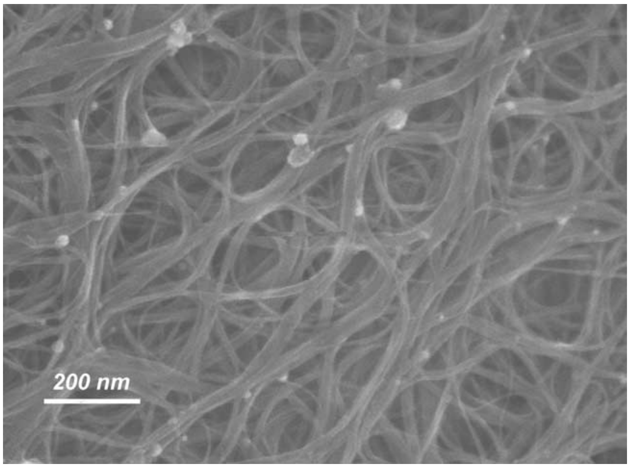

Fig. 5. An SEM image of the PKS-functionalized SWNT sample after thermal defunctionalization in TGA scan.

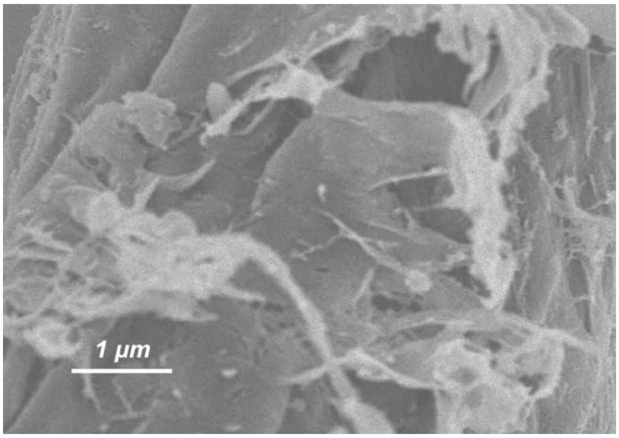

Fig. 6. An SEM image of the PKS-functionalized SWNT sample after the chemical defunctionalization.

nanotube content in the sample was estimated to be ∼20 wt% (Fig. 4). On the other hand, TGA was also used to evaluate the insoluble residue from the functionalization reaction. Before the analysis, the residue sample was washed repeatedly with THF, in which PKS is highly soluble, to remove any unattached PKS. According to the result shown in Fig. 4, the polymeric functional groups accounted for 20–30 wt% of the insoluble residue. These PKS species were likely attached to those nanotubes that were insufficiently functionalized to attain solubility.

The functionalization reaction was under conditions designed for the esterification of the nanotube surface-bound carboxylic acids. There has been little success in literature to provide direct evidence on such a mode of functionalization [32,39]. Nevertheless, indirect evidence may be obtained from the chemical defunctionalization to hydrolyze the ester linkages [33]. The defunctionalization of the PKS-functionalized SWNTs was achieved under the reaction conditions for acid-catalyzed hydrolysis, resulting in the precipitation of the defunctionalized nanotubes. The remaining solution became much less colored, consistent with the removal of nanotubes. According to the SEM analysis of the recovered nanotube sample (Fig. 6), the defunctionalization was incomplete, namely that the precipitated were mostly under-functionalized SWNTs as a result of the partial removal of the polymeric functional groups [16,18,32,33]. There was apparently a significant amount of soft materials (remaining PKS polymers) in the SEM specimen.

The shared solubility of PKS-functionalized SWNTs with PVK homopolymer in chlorobenzene allowed their intimate mixing in solution (Fig. 7). The selection of chlorobenzene as a solvent for wet-casting was for its intermediate boiling point (thus suitable vapor pressure under ambient conditions). The PVK-SWNT nanocomposite thin film on the ITO-coated glass substrate appeared homogeneous and optically transparent. The film contained around 3 wt% of SWNTs, estimated from the nanotube content in the PKS-functionalized SWNT sample.

The charge dissipation properties of the PVK-SWNT nanocomposite thin film (less than 1 μm in thickness and highly transparent) in the dark and under the illumination of white light were compared. The film surface was charged by a corona in the charge decay test unit, followed by monitoring the charge decay. As shown in Fig. 8, the decay was much faster under the illumination than in the dark, with $\vartheta_{\text{light}} \sim 0.7$ s vs. $\vartheta_{\text{dark}} \sim 1.4$ s, where ϑ represents the time for the surface charge to decay to $1/e$ of the initial value. It should be noted that the charge decay in the dark is relatively fast, in comparison with that in neat PVK film, which was likely due to the presence of conductive nanotubes (metallic SWNTs, in particular) as well-dispersed fillers in the nanocomposite film.

PVK is a well-known hole-transport polymeric material. The dispersion of SWNTs in PVK matrix apparently enhances the charge dissipation under photo-illumination [6]. In nanotubes themselves, photoconductivity has been observed and investigated [40–45]. However, the role of nanotubes in the PVK-SWNT nanocomposite here might be as photoinduced charge generators (like C_{60} in PVK matrix), but the mechanistic details on such activities remain to be explored in further investigations.

In summary, a specifically designed PVK copolymer with pendant hydroxyl groups was synthesized and used to functionalize SWNTs, yielding a soluble functionalized SWNT sample. The sample was thoroughly characterized by using various spectroscopic and microscopic methods. The solubility of PKS-functionalized SWNTs in the same solvent for PVK homopolymer enabled well-mixing in solution and the subsequent spin-casting of the PVK-SWNT nanocomposite thin film of a high optical quality. The charge dissipation in the nanocomposite was apparently enhanced under light illumination. A more systematic experimental investigation on the role of well-dispersed carbon nanotubes in charge generation and transportation in PVK polymer matrix is planned.

Fig. 7. Chlorobenzene solutions of PKS-functionalized SWNTs and PVK homopolymer mixtures with nanotube contents of ~3 wt% (left) and ~0.1 wt% (right) before spin-casting.

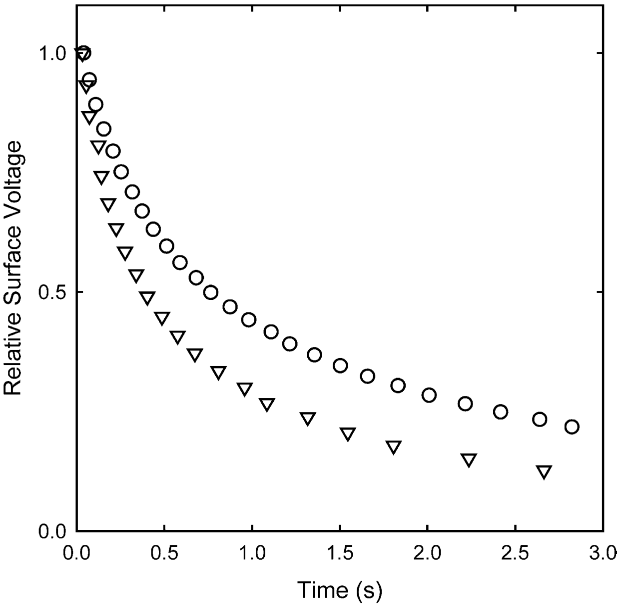

Fig. 8. Charge decays of the PKS-SWNT nanocomposite thin film in dark (○) and under illumination of white light (▽).

Acknowledgements

We thank Prof A.M. Rao for supplying carbon nanotube samples, Dr B. Chen for AFM measurement, and S. Fernando, D. Hill, H. Li, L. Qu, and B. Zhou for experimental assistance. Financial support from NASA, NSF, and the Center for Advanced Engineering Fibers and Films (NSF-ERC at Clemson University) is gratefully acknowledged.

References

[1] Law KY. Chem Rev 1993;93(1):449–86.
[2] Winiaz JG, Zhang L, Lal M, Friend CS, Prasad PN. J Am Chem Soc 1999;121(22):5287–95.
[3] Wang Y. Nature 1992;356(6370):585–7.
[4] Yoshino K, Kajii H, Araki H, Sonoda T, Take H, Lee S. Fullerene Sci Technol 1999;7(4):695–711.
[5] Lee SB, Katayama T, Kajii H, Araki H, Yoshino K. Synth Met 2001; 121(1–3):1591–2.
[6] Wu W, Li J, Liu L, Yanga L, Guo ZX, Dai L, et al. Chem Phys Lett 2002;364(1–2):196–9.
[7] Wu W, Zhang S, Li Y, Li J, Liu L, Qin Y, et al. Marcomolecules 2003; 36(17):6286–8.
[8] Cao L, Chen H, Wang M, Sun J, Zhang X, Kong F. J Phys Chem B 2002;106(35):8971–5.
[9] Kim JY, Kim M, Kim HM, Joo J, Choi JH. Opt Mater 2002;21(1–3): 147–51.
[10] Kim JY, Kim M, Choi JH. Synth Met 2003;139(3):565–8.
[11] Mulazzi E, Perego R, Aarab H, Mihut L, Lefrant S, Faulques E, et al. Phys Rev B 2004;70(15):155206.
[12] Valentini L, Armentano I, Kenny JM, Bidali S, Mariani A. Thin Solid Films 2005;476(1):162–7.
[13] Tang BZ, Xu H. Macromolecules 1999;32(8):2569–76.
[14] Barraza HJ, Pompeo F, O'Rear EA, Resasco DE. Nano Lett 2002; 2(8):797–802.
[15] Grady BP, Pompeo F, Shambaugh RL, Resasco DE. J Phys Chem B 2002;106(23):5852–8.
[16] Hill DE, Lin Y, Rao AM, Allard LF, Sun YP. Macromolecules 2002; 35(25):9466–71.
[17] Hill DE, Lin Y, Allard LF, Sun YP. Int J Nanosci 2002;1(3–4): 213–21.
[18] Lin Y, Zhou B, Fernando KAS, Liu P, Allard LF, Sun YP. Macromolecules 2003;36(19):7199–204.
[19] Qu LW, Lin Y, Hill DE, Zhou B, Wang W, Sun X, et al. Macromolecules 2004;37(16):6055–60.
[20] Fernando KAS, Lin Y, Zhou B, Grah M, Joseph R, Allard LF, et al. J Nanosci Nanotechnol, 2005;5(7):1050–4.
[21] Viswanathan G, Chakrapani N, Yang H, Wei B, Chung H, Cho K, et al. J Am Chem Soc 2003;125(31):9258–9.
[22] Yao Z, Braidy N, Botton GA, Adronov A. J Am Chem Soc 2003; 125(51):16015–24.
[23] Kong H, Gao C, Yan D. J Am Chem Soc 2004;126(2):412–3.
[24] Qin S, Qin D, Ford WT, Resasco DE, Herrera JE. J Am Chem Soc 2004;126(1):170–6.
[25] Liu IC, Huang HM, Chang CY, Tsai HC, Hsu CH, Tsiang RCC. Macromolecules 2004;37(2):283–7.
[26] Blake R, Gun'ko YK, Coleman J, Cadek M, Fonseca A, Nagy JB, et al. J Am Chem Soc 2004;126(33):10226–7.
[27] Sen R, Zhao B, Perea D, Itkis ME, Hu H, Love J, et al. Nano Lett 2004;4(3):459–64.
[28] Gao JB, Itkis ME, Yu A, Bekyarova E, Zhao B, Haddon RC. J Am Chem Soc 2005;127(11):3847–54.
[29] Journet C, Maser WK, Bernier P, Loiseau A, de la Chapelle ML, Lefrant S, et al. Nature 1997;388(6644):756–8.
[30] Liu J, Rinzler AG, Dai HJ, Hafner JH, Bradley RK, Boul PJ, et al. Science 1998;280(5367):1253–6.
[31] Chen J, Hamon MA, Hu H, Chen Y, Rao AM, Eklund PC, et al. Science 1998;282(5386):95–8.
[32] Sun YP, Huang W, Lin Y, Fu K, Kitaygorodskiy A, Riddle LA, et al. Chem Mater 2001;13(9):2864–9.
[33] Fu K, Huang W, Lin Y, Riddle LA, Carroll DL, Sun YP. Nano Lett 2001;1(8):439–41.
[34] Riggs JE, Guo Z, Carroll DL, Sun YP. J Am Chem Soc 2000;122(24): 5879–80.

[35] Sun YP, Zhou B, Henbest K, Fu K, Huang W, Lin Y, et al. Chem Phys Lett 2002;351(5–6):349–53.
[36] Guldi DM, Holzinger M, Hirsch A, Georgakilas V, Prato M. Chem Commun 2003;(10):1130–1.
[37] Sun YP, Fu K, Lin Y, Huang W. Acc Chem Res 2002;35(12):1096–104.
[38] O'Connell MJ, Bachilo SM, Huffman CB, Moore VC, Strano MS, Haroz EH, et al. Science 2002;297(5581):593–6.
[39] Hamon MA, Hui H, Bhowmik P, Itkis HME, Haddon RC. Appl Phys A 2002;74(3):333–8.
[40] Fujiwara A, Matsuoka Y, Suematsu H, Ogawa N, Miyano K, Kataura H, et al. Jpn J Appl Phys Part 2—Lett 2001;(11B):L1229–L31.
[41] Freitag M, Martin Y, Misewich JA, Martel R, Avouris P. Nano Lett 2003;3(8):1067–71.
[42] Levitsky IA, Euler WB. Appl Phys Lett 2003;83(9):1857–9.
[43] Balasubramanian K, Fan Y, Burghard M, Kern K, Friedrich M, Wannek U, et al. Appl Phys Lett 2004;84(13):2400–2.
[44] Fujiwara A, Matsuoka Y, Matsuoka Y, Suematsu H, Ogawa N, Miyano K, et al. Carbon 2004;42(5/6):919–22.
[45] Khairoutdinov RF, Doubova LV, Haddon RC, Saraf L. J Phys Chem B 2004;108(52):19976–81.